nature communications

Article

https://doi.org/10.1038/s41467-024-52976-1

Rewiring native post-transcriptional global regulators to achieve designer, multi-layered genetic circuits

Received: 14 May 2024

Accepted: 27 September 2024

Published online: 09 October 2024

Check for updates

Trevor R. Simmons[1], Gina Partipilo[1], Ryan Buchser[1], Anna C. Stankes[1], Rashmi Srivastava[2], Darian Chiu[1], Benjamin K. Keitz[1] & Lydia M. Contreras[1]

As synthetic biology expands, creating "drag-and-drop" regulatory tools that can achieve diverse regulatory outcomes are paramount. Herein, we develop a approach for engineering complex post-transcriptional control by rewiring the Carbon Storage Regulatory (Csr) Network of *Escherichia coli*. We co-opt native interactions of the Csr Network to establish post-transcriptional logic gates and achieve complex bacterial regulation. First, we rationally engineer RNA-protein interactions to create a genetic toolbox of 12 BUFFER Gates that achieves a 15-fold range of expression. Subsequently, we develop a Csr-regulated NOT Gate by integrating a cognate 5′ UTR that is natively Csr-activated into our platform. We then deploy the BUFFER and NOT gates to build a bi-directional regulator, two input Boolean Logic gates OR, NOR, AND and NAND and a pulse-generating circuit. Last, we port our Csr-regulated BUFFER Gate into three industrially relevant bacteria simply by leveraging the conserved Csr Network in each species.

There is a need in synthetic biology for genetic toolkits that provide "drag and drop" components that allow for tuning of synthetic processes or metabolic pathways with minimal part optimization. It is critical these "drag and drop" toolkits perform complex genetic logic and can be ported into multiple different species of industrially relevant organisms[1]. Most synthetic bacterial control systems rely on engineered genetic components that are expressed at much higher concentration compared to their native regulatory networks and operate orthogonally from host function. The dysregulation between synthetic and native components imposes a metabolic burden and can limit the performance of an engineered system[2,3]. As system complexity increases, the potential for system failure also increases as many synthetic systems rely on disparate parts, which work tangentially and often operate inefficiently together[4]. There is a need to develop systems with fewer genetic parts that do not compromise the processing capabilities of the engineered system. One way to do this is to design toolkits that co-opt native cell regulation machinery to achieve their desired regulation.

Recently, post-transcriptional control has been identified as a scheme for reducing metabolic burden in synthetic systems, as the cost-per protein within the cell is lessened[5–8]. Post-transcriptional regulation has been an effective approach for coordinating synthetic regulation with native regulatory machinery. Historically, post-transcriptional networks that serve as effective scaffolds for engineered regulation possess well-characterized interactions and multiple nodes for tunability[9–11]. These engineered tools established a strong foundation for using native systems as a scaffold. Moving forward, it is paramount to develop tools that can perform complex computation (i.e., respond to multiple inputs), as well as achieve an array of well-defined regulatory outcomes (i.e., activation, repression, pulse, etc.).

One post-transcriptional network that fits the regulation criteria is the bacterial Carbon Storage Regulatory system (Csr) System, also known as the Regulator of Secondary Metabolites (Rsm) System. The Csr Network is a post-transcriptional regulatory cascade (Fig. 1A) native to *E. coli* and is conserved throughout many bacterial classes[12]. The main regulator is Carbon Storage Regulatory Protein A (CsrA), a

[1]McKetta Department of Chemical Engineering, The University of Texas at Austin, Austin, TX 78712, USA. [2]Department of Chemistry and Biochemistry, Baylor University, Waco, TX 76706, USA. e-mail: lcontrer@che.utexas.edu

https://doi.org/10.1038/s41467-024-52976-1

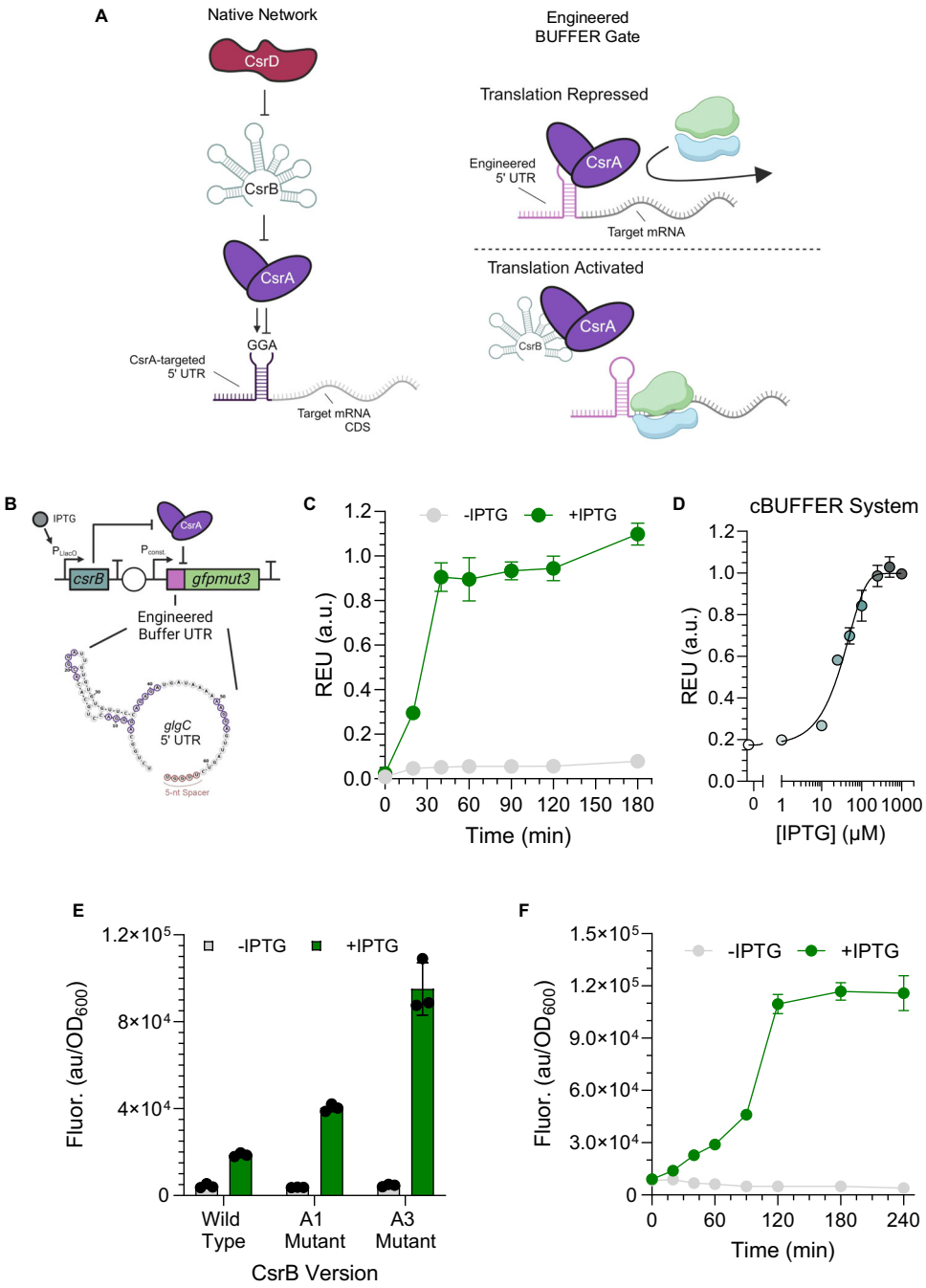

Fig. 1 | Development of the Proof-of-concept Csr-regulated BUFFER Gate (cBUFFER). A Native post-transcriptional interactions of the Csr Network (left), and the hypothesized engineered system (right). In the engineered BUFFER Gate, natively expressed CsrA repressed a synthetic target through an engineered 5′ UTR sequence, and target translation is activated through induction of the sponge sRNA, CsrB. **B** Genetic circuit diagram of cBUFFER – the target of interest *gfpmut3* is repressed by CsrA through the engineered *glgC* 5′ UTR sequence and CsrB transcription is activated through IPTG induction. These genetic components were expressed from a ColE1 ori-based plasmid (Copy Number 10–15). **C** Time course of initial cBUFFER fluorescence for induced (+ IPTG) and uninduced (-IPTG). The initial cBUFFER utilized the wild type CsrB sequence. **D** Titration response curve of initial cBUFFER fluorescence two hours post-induction. **E.** Fluorescence of cBUFFER systems using different versions of the CsrB sRNA. Mutants A1 and A3 contain deletions of the RNase E degradation site initially identified in Vakulskas et al. 2016 *NAR*. F Time course of optimized cBUFFER fluorescence for induced (+ IPTG) and uninduced (-IPTG) samples. The optimized version uses the CsrB A3 mutant. Samples were grown in biological triplicate, and data presented are the mean values +/- the standard deviation, represented as the error bars.

global RNA-Binding Protein (RBP) implicated in regulating dozens of mRNA transcripts[13–16]. Canonically, CsrA regulates mRNA targets through binding an A(N)GGA motif (referred to as the "GGA Motif" hereafter) within a stem-loop of an RNA hairpin in the 5′ Untranslated Region (5′ UTR) of the transcript[17]. The RBS is occluded by CsrA via binding to the GGA Motif in the UTR and preventing binding of the 30S subunit[18]. Regulation of the CsrA protein occurs via two sRNAs, CsrB and CsrC, which bind up to 9 and 5 copies of CsrA, respectively, as the sRNAs consist of several hairpins containing the GGA Motif[19]. These sRNAs are regulated by the protein CsrD, which facilitates the degradation of the two sRNAs with RNAse E[20]. Importantly, the topology of this network natively performs dynamic bacterial computation in response to different cellular and environmental signals[13,21].

Taking these factors into account, we identified the Csr Network as a prime candidate to serve as a scaffold for engineered post-transcriptional regulation. Herein, we rewire native regulatory interactions of the Csr Network to build multi-layered, modular genetic circuits. We leverage the unique capabilities of this network to achieve complex and unique bacterial computation. Our system focuses on precisely controlling the CsrB sRNA, which recruits the CsrA protein and thereby allows for the modulation of CsrA-mRNA interactions. Furthermore, this native regulatory network bridges the gap to higher-order regulation through the CsrD protein, which modulates CsrB sRNA degradation. To activate our synthetic system, we overexpressed the CsrB sRNA from a plasmid, which sequesters bound native CsrA away from our engineered UTRs. Using two cognate 5′ UTRs we established both a CsrA-regulated BUFFER and NOT Gate. We then improved system tunability by rationally engineering the RBS and CsrB sequences to achieve a 15-fold range of signal response. Next, leveraging the BUFFER and NOT Gates, we developed CsrA-CsrB regulated OR, NOR, AND, and NAND Boolean Logic Gates. We then applied the unique regulatory capabilities of the Csr Network to create a bi-directional regulation within a single operon, a genetic pulse circuit integrating the full Csr cascade, and a nested three input-two output OR-AND hybrid Gate. Lastly, we showed the CsrA-regulated BUFFER Gate could function across multiple industrially relevant bacteria with minimal optimization by leveraging the native Csr Network in each species. Overall, these results demonstrate the potential of repurposing the Csr Network as an engineered scaffold for regulation and support the notion that native post-transcriptional networks can be co-opted for complex and unique bacterial computation.

Results

Developing a buffer gate via native CsrA control

We chose to leverage the constitutive, intracellular native expression of CsrA in the *E. coli* to directly control mRNA transcripts[13]. We first sought to construct a CsrA-CsrB regulated BUFFER Gate by fusing a 5′ UTR from a CsrA natively repressed mRNA transcript target where bound CsrA occludes the RBS. This repurposed CsrA to repress a synthetic target through its canonical repression mechanism. To activate the Buffer Gate the sRNA, CsrB, would be expressed to sequester CsrA from the UTR of our synthetic target and to allow translation of the target mRNA to occur (Fig. 1A). We termed this CsrA-CsrB regulated BUFFER Gate "cBUFFER". To create the synthetic components required for cBUFFER, we selected the 5′ UTR from the *glgC* transcript as our 5′ UTR of interest for multiple reasons: the CsrA binding sites in the *glgC* 5′ UTR are well-documented[18,22]; CsrA is the only known protein or RNA that binds the *glgC* 5′ UTR; and previous literature has shown that CsrA represses the *glgC* transcript with the greatest fold-strength in vivo compared to other 5′ UTR sequences (15- to 20-fold, compared to 2- to 5-fold for other confirmed and putative targets[13]). CsrA preferentially binds the *glgC* 5′ UTR at two primary GGA-motif sites: one in the stem loop, and one in the native ribosome binding site. There are also secondary binding sites in a GGA-motif directly upstream of the hairpin, and an AGAGA motif directly downstream of the hairpin[14,18]. We selected the *glgC* -61 to -1 sequence relative to the native translation start site for the engineered 5′ UTR scaffold, as it is the minimal sequence containing the hairpin and all CsrA binding sites (Fig. 1B). We added the five nucleotide "TTGGT" spacer to the 3′ end of the UTR sequence to provide future ribosome binding site tunability. We selected to append five nucleotides as it the maximum base pair length that did not disrupt the predicted native secondary structure of the GGA Motif-containing stem loop, as per ViennaRNA secondary structure predictions. (Supp Fig. S1). As our gene of interest, we selected *gfpmut3* for detection via fluorescent screening. We placed this fusion transcript under the P_{Con12} promoter, a weak constitutive promoter previously used in studying bacterial post-transcriptional networks[23]. Next, we placed the wild-type CsrB sequence under the P_{LlacO} promoter to be inducible via isopropyl β-D-1-thiogalactopyranoside (IPTG). Specifically, the P_{LlacO} promoter is controlled by the LacI regulatory protein derived from the native *lacI* sequence of the K-12 MG1655 strain of *E. coli*, as previously established in work by Lutz and colleagues[24]. These two genetic components were expressed on a single ColE1 origin of replication plasmid (Fig. 1B). We expected that upon induction, the CsrB sRNA would sequester CsrA away from the *glgC* 5′ UTR-*gfpmut3* fusion transcript, allowing for translation and generating a fluorescent signal.

We observed a rapid fluorescent signal accumulation within 20 minutes and saturation within 40–60 minutes post-induction (Fig. 1C). We also tested the tunability of the system by titrating CsrB expression at different IPTG induction concentrations, and found the system provides tunability between 10–1000 μM IPTG. Additionally, the titratability of the cBUFFER systems is comparable to that of a P_{LlacO}, IPTG-inducible transcriptional BUFFER Gate (Supplementary Fig. S2). Importantly, no growth defects were observed for the induced samples compared to the uninduced samples (Supplementary Figure S3), demonstrating that the conditions selected for CsrB expression do not disrupt cell viability or growth due to sequestration of CsrA.

To confirm that CsrA is responsible for interacting with the engineered *glgC* 5′ UTR sequence and repressing translation, we tested cBUFFER in a *csrA::kan* strain and found that there was minimal activation of the Buffer Gate upon CsrB induction (Supplementary Fig. S4). Additionally, we mutated the CsrA binding sites in the engineered *glgC* 5′ UTR to inhibit function and tested this mutant construct in wild-type *E. coli*, as well as in the *csrA::kan* strain. In both strains, we did not observe any change in expression between the induced and uninduced samples (Supplementary Figure S4). These results supported that the interaction behind cBUFFER is driven by CsrA repressing translation of the *gfpmut3* mRNA transcript through interactions with the engineered 5′ UTR.

This preliminary design yielded approximately 8-fold activation when comparing the relative signal between the uninduced and induced states. While promising, we wanted to improve the activation in cBUFFER. Additionally, in some cases fluorescent signal would decrease after beyond three hours. We thought this was due to the fact the CsrB sRNAs were being degraded by RNase E. To reduce this, we evaluated two mutations to the RNase E degradation site in the CsrB sRNA, previously shown to reduce RNase E activity on CsrB[25]. The first mutation, termed A1, is a deletion of the second and third nucleotides in the RNase E binding site. The second mutation, A3, deleted the fifth and sixth nucleotides in the RNase E binding site. When integrated into cBUFFER, we observed a 10-fold increase in GFP signal activation for the A1 mutant, and a 20-fold increase for the A3 mutant (Fig. 1E). Moving forward we elected to use the A3 mutant, as it maximized signal amplification (Fig. 1F). The A3 mutant CsrB showed slower activation compared to the WT CsrB sequence, which could have been due to changes in secondary structure folding from to the mutations in the RNAse E binding region. Overall, this circuit still achieved full activation within 90-120 minutes post-induction. The premise of using an inducible CsrB-CsrA-5′UTR as part of a basic translational reporter of transcripts that are regulated by CsrA was previously demonstrated in our work in the context of the native 5′ UTR plus 100 nucleotides of the coding sequence of several potential native CsrA targets[13,16]. This work extends this basic premise into the synthetic realm by developing a fully cognate 5′ UTR sequence that contains a minimal CsrA-binding region as well as a tunable RBS handle through the 5-nucleotide spacer that can be used to regulate any synthetic target by CsrA. Additionally, we identified an optimized CsrB sRNA sequence to maximize its ability to sequester CsrA.

https://doi.org/10.1038/s41467-024-52976-1

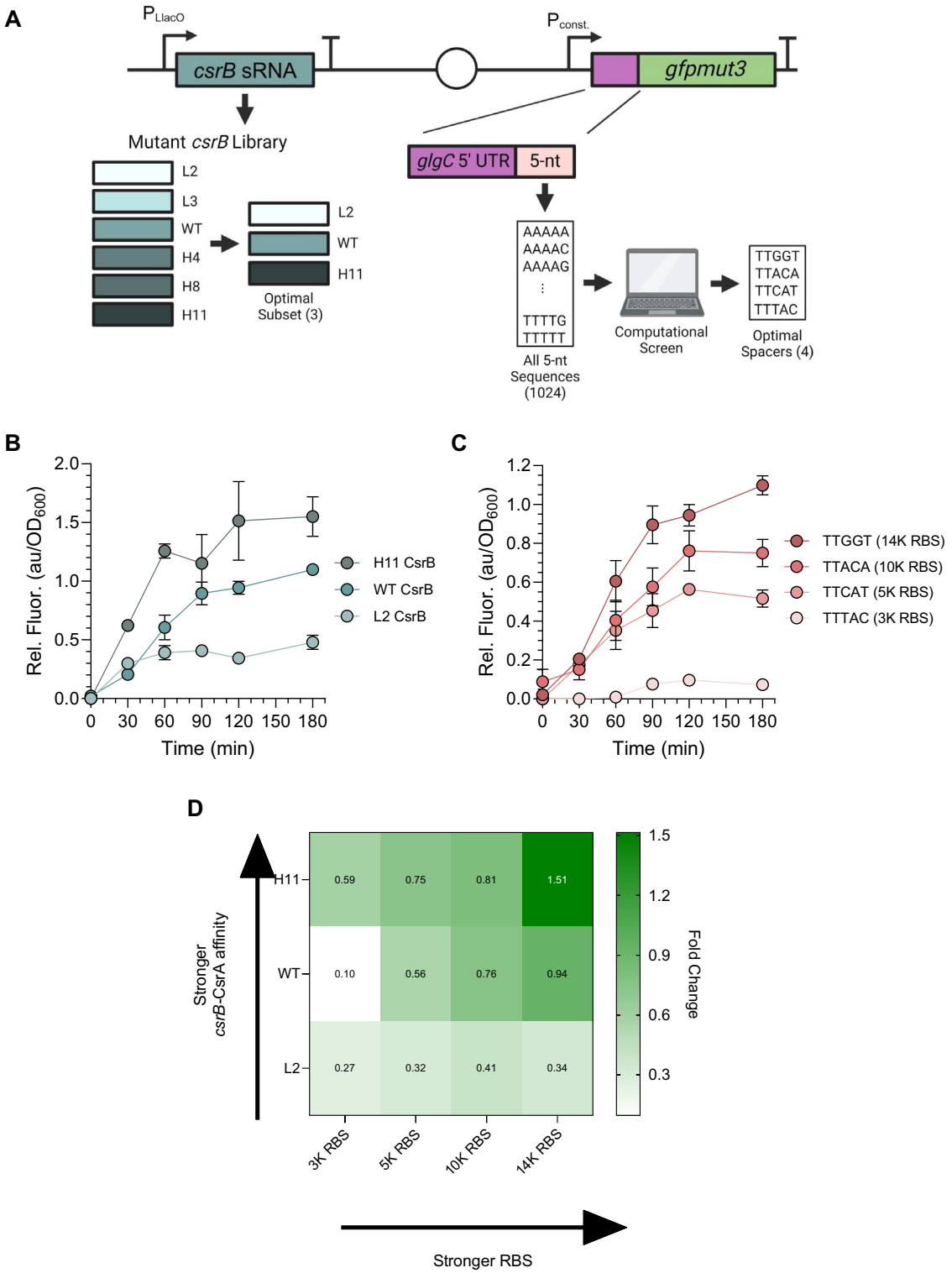

Fig. 2 | Expanding tunability of the cBUFFER through RBS strength and CsrB-CsrA affinity modulation. A Workflow for tuning cBUFFER expression. To tune CsrA-CsrB affinity, mutant CsrB sequences containing mutations to known CsrA binding sites were tested. To vary RBS strength, all 1024 five nucleotide space sequences were computationally screened, resulting in 4 additional optimized sequences. **B** Time course of cBUFFER systems with variable CsrB sRNAs; WT CsrB (Blue), High-affinity CsrB (Dark Blue), and Low-affinity mutant CsrB L2 (Light Blue). **C** Time course of cBUFFER systems with variable RBS strengths derived from the computational screen. **D** Relative fluorescence for all combinations of RBS-CsrB cBUFFER systems, two hours post-induction. Samples were grown in biological triplicate, and data presented are the mean values +/- the standard deviation, represented as the error bars.

Tuning CsrA-CsrB Affinity and RBS strength to expand tunability of gene expression in cBUFFER

After validating and optimizing cBUFFER, we sought to expand the tunability beyond CsrB titration through IPTG. In evaluating the tunable nodes of our system, we identified that we could tune the interactions between CsrA and CsrB, as well as the RBS strength of our target genes in cBUFFER (Fig. 2A). We replaced the original CsrB sRNA sequence with engineered CsrB mutants previously established in our

lab[26] that altered the in vivo affinity between CsrA and CsrB. We selected five CsrB sequences that previously demonstrated a range of 0.7 to 3.5-fold change CsrB-CsrA affinity relative to the wild-type CsrB-CsrA interaction. Of the five CsrB sRNAs tested, we chose to use the CsrB L2 and H11[26] which achieved a 0.5-fold and 1.4-fold change in signal activation, relative to the original cBUFFER (Fig. 2B). It is worth noting that, when tested, the remaining CsrB mutants demonstrated either minimal difference in signal change relative to the original cBUFFER or introduced significant growth defects (Supplementary Figure S5).

Next, we evaluated the ability to tune RBS strength by varying the 5-nt spacer sequence at the 3′ end of the engineered UTR. To do so, we first considered all remaining possible combinations of five nucleotide sequences from AAAAA to TTTTT, which yielded 1023 possible spacers (4^5 combinations or 1024, excluding the original TTGGT). Next, we eliminated any spacers containing the GGA motif to not introduce new potential CsrA binding sites, leaving us with 974 spacer candidates. These were screened for predicted RBS strength via the Salis RBS Calculator 2.0[27]. Then eliminated sequences that had translation rates of approximately zero, yielding 959 candidates. From this subset, we evaluated predicted secondary structure of each engineered 5′ UTR, the *glgC* 5′ UTR plus 5 nucleotide spacer, using RNAfold from ViennaRNA (http://rna.tbi.univie.ac.at/cgi-bin/RNAWebSuite/RNAfold.cgi). We selected only the candidates that did not change in secondary structure compared to that of the wild type *glgC* 5′ UTR sequence. This yielded a final subset of 65 sequences; we picked and experimentally screened four sequences that maximize the range of predicted RBS strengths (Fig. 2C). Three of the four constructs tested generated measurable GFP expression in cBUFFER that correlated with predicted RBS strength (Fig. 2C). One of the four spacers did not generate detectable GFP signal (Supp. Fig. S6). Importantly, each working construct demonstrated similar fold-activation upon induction as observed in the original cBUFFER, reinforcing that these new spacers do not affect CsrA regulation in the 5′ UTR (Fig. 2C, Supplementary Figure S6). Finally, we combined the cBUFFER Gates with the mutant CsrB sRNAs with those containing the new spacers to create a total of12 iterations of the cBUFFER Gate that achieve a 15-fold range of tunable expression (Fig. 2D, Supplementary Figure S7. Moving forward, inducer concentration, RBS strength, and CsrA-CsrB affinity can now all be utilized to tune target gene expression from the cBUFFER constructs.

Evaluating multi-gene regulation in cBUFFER

Next, we investigated the capabilities of cBUFFER to regulate genes beyond *gfpmut3*. To start, we replaced *gfpmut3* in cBUFFER (Fig. 1), with *mcherry* and *eyfp* and observed consistent activation upon induction for each of these new target genes (Fig. 3A). Next, we evaluated if cBUFFER could regulate all three genes simultaneously on separate plasmids within the same organism. Each 5′ UTR-fluorescent protein fusion plasmid was transformed into the same strain, and we observed that cBUFFER successfully regulated all three targets simultaneously with similar signal activation to that of each individual target (Fig. 3B). These results demonstrate that the native CsrA expressed is sufficient to regulate up to three synthetic targets simultaneously, and still perform required cellular functions.

We then sought to establish if cBUFFER could regulate three genes on a single transcript. To test this, we constructed a synthetic operon containing *gfpmut3*, *mcherry*, and *eyfp* each containing the engineered 5′ UTR sequence (Fig. 3C). Using the synthetic operon, we observed signal activation for each gene in the operon upon CsrB induction (Fig. 3D). All three genes reached the same level of activation in the synthetic operon to that of both the individual and triple plasmid approach. We then evaluated if we could tune the individual expression of each gene within the operon. This was done by implementing the engineered 5′ UTRs containing the various RBS spacers established above. We replaced the original engineered 5′ UTR (14 K RBS) upstream of *gfpmut3* with the 5′ UTR containing the weakest strength RBS (3 K RBS). We also replaced the 5′ UTR upstream of *mcherry* with the engineered 5′ UTR containing the intermediate strength RBS (10 K RBS). Upon induction of CsrB, we observed a proportional reduction in signal for GFP and mCherry that corresponded with the 5′ UTR RBS strength upstream of each gene (Fig. 3D). The EYFP signal remained consistent to that observed in the previous experiments. These data confirm that the design rules for RBS tunability established in the single cBUFFER cases transfer to multi-target and synthetic operon designs. Moreover, individual gene expression can be predictively tuned independently within a synthetic operon.

Integrating non-canonical CsrA-regulated 5′ UTR creates a Csr-regulated NOT Gate (cNOT) and higher order multi-input Logic Gates

With cBUFFER established, we then sought to develop a Csr-regulated NOT Gate (cNOT), which would allow for repression of a target gene upon induction of CsrB. This would allow for this Csr-based regulation to achieve both single Boolean Logic Gates, expanding the potential for additional complexity in future gate designs. To this end, we applied the use of a natively occurring 5′UTR of an mRNA sequence that is activated for translation upon CsrA binding and therefore translation is attenuated by sequestering CsrA via CsrB. Specifically, we focused on the studied *ymdA* 5′ UTR transcript, which exhibits CsrA-dependent translation activation[28]. The *ymdA* 5′ UTR consists of two GGA motifs and the RBS contained within a hairpin structure. When CsrA binds to the *ymdA* hairpin, the hairpin structurally rearranges to release the RBS, allowing for translation initiation (Fig. 4A). Therefore, available of free CsrA activates expression of the target gene. To evaluate if this 5′ UTR sequence could be inserted into the synthetic gate design and invert the logic of the system, we replaced the *glgC* sequence (naturally bound by CsrA to repress translation of its adjacent mRNA) with the -58 to -1 *ymdA* 5′ UTR sequence (Fig. 4B). In our new design, we observed a rapid reduction in GFP signal upon induction of CsrB, which ultimately reached a 6-fold reduction in signal after 2 hours. With this new 5′ UTR sequence, we established a Csr-regulated NOT Gate or the cNOT system. Importantly, the only difference between cBUFFER and cNOT was the 58nt sequence of the 5′ UTR region; the remaining structure of the plasmid remained unchanged.

Next, we investigated if cNOT could be deployed in parallel with cBUFFER to achieve concurrent bi-directional regulatory outcomes. To do this, we placed GFP under control of cNOT Gate and mCherry under control of cBUFFER on separate plasmids to first evaluate whether orthogonal logics could be controlled within a single cell (Fig. 4D). We observed 4-fold activation of mCherry signal and 3-fold repression of GFP signal after induction (Fig. 4D, E), demonstrating that our gates can be used in parallel to achieve diverging regulatory outcomes driven by the CsrA-5′ UTR interaction. Creating a diverging regulator on a single synthetic operon emphasizes the capabilities specific to this network, modulation of the 5′UTR region of the gene of interest can diverge behavior. We therefore placed the cNOT and cBUFFER 5′ UTRs and target genes on a single synthetic operon, such that CsrA could regulate both targets on a single sequence to achieve diverging outcomes (Fig. 4G). Using this approach, the inducible CsrB can exert control of orthogonal logics without any additional regulatory elements introduced to the system, and we observed a 10-fold reduction in GFP signal and 8-fold increase in mCherry signal 2 hours after CsrB induction via IPTG (Fig. 4H, I).

With cBUFFER and cNOT established, we expanded the capabilities of this approach to two-input Boolean Logic Gates, specifically the OR, NOR, AND, and NAND Gates by leveraging the cBUFFER and cNOT system architectures and placing CsrB under multiple regulators. First, we constructed a Csr-regulated OR Gate, termed cOR, by

https://doi.org/10.1038/s41467-024-52976-1

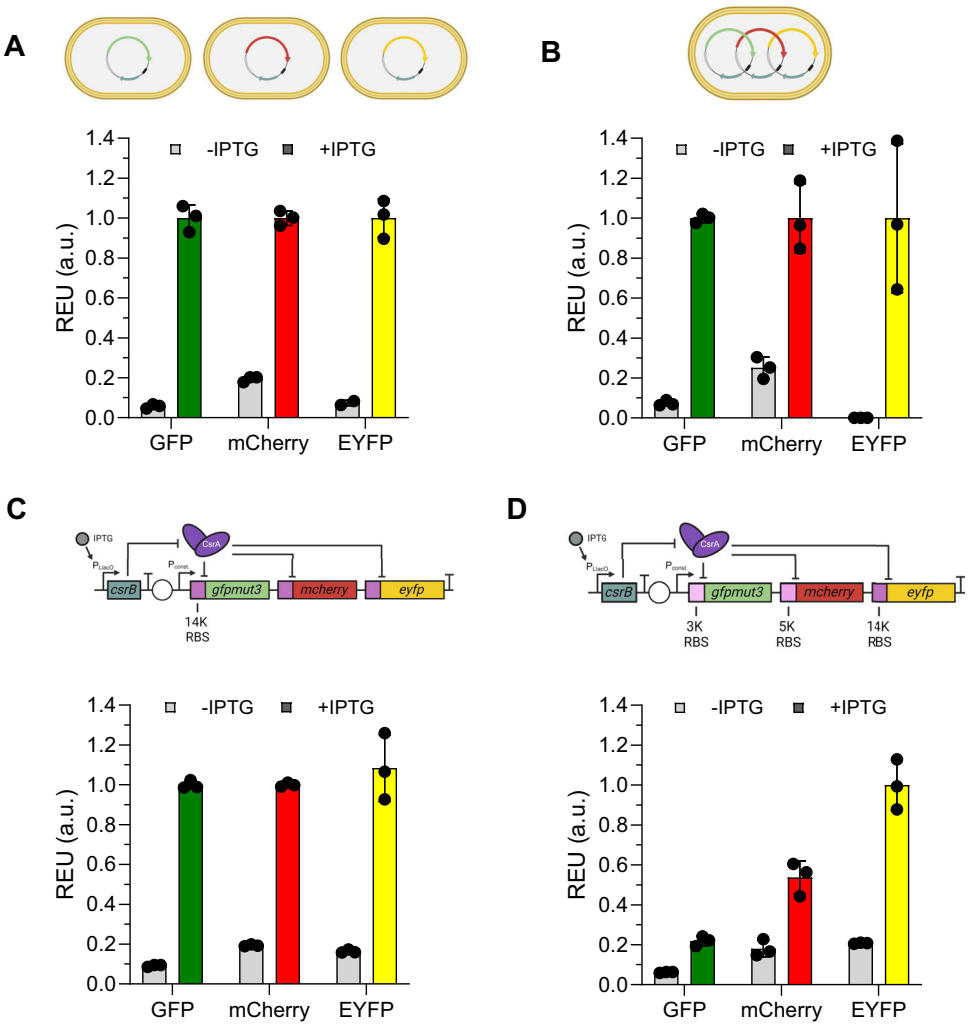

Fig. 3 | Evaluating cBUFFER capabilities to regulate multiple genes. A Relative expression of GFP, mCherry, and EYFP in individual cBUFFER systems two hours post-induction. **B** Relative expression of GFP, mCherry, and EYFP in a single cBUFFER, two hours post-induction. **C** Relative expression of GFP, mCherry, and EYFP two hours post-induction regulated in a single synthetic operon with each target gene fused to the engineered 5′ UTR containing the strongest RBS. **D** Relative expression of GFP, mCherry, and EYFP two hours post-induction. Each gene in the operon had a different RBS strength via the engineered 5′ UTR upstream of each gene. Samples were grown in biological triplicate, and data presented are the mean values +/- the standard deviation, represented as the error bars.

placing the CsrB sRNA under TetR and LacI regulation, while keeping the engineered *glgC* 5′ UTR sequence the same. Similar to the LacI regulator protein, TetR is natively derived from the K-12 strain of *E. coli*[29], and used in combination with the P_{LTetO} promoter previously established[24]. We expected to observe signal activation in the presence of either anhydrotetracycline (aTc) or IPTG, or both compounds (Fig. 5A). These expected results were confirmed with the cOR system achieving approximately 8-fold activation. We also constructed a Csr-regulated NOR Gate, cNOR, by integrating the engineered *ymdA* 5′ UTR, maintaining identical architecture with flipped logical outcomes by changing only the 5′ UTR. We expected cNOR to follow the inverse logic of cOR, a loss of signal in the presence of either aTc or IPTG or both compounds. Again, our expected results were confirmed in vivo, as the Csr-regulated NOR Gate achieved a 2-fold reduction upon CsrB induction (Fig. 5B).

Next, we designed Csr-regulated AND and NAND Gates, termed cAND and cNAND, in similar fashion to the cOR and cNOR Gates. For these two Gates however, we instead placed CsrB expression under AraC and TetR regulation. As a note, the AraC regulator protein was derived from K-12 *E. coli* established by Johnson and colleagues[30]. The Arac regulator is used in with the P_{BAD} promoter, with sequences derived from previous works ([30] and BioBrick part BBa_I0500). We constructed these gates such that CsrB was downstream of the P_{araBAD} and P_{LTetO} promoters in series, predicting that CsrB could only be expressed when both L-arabinose (L-ara) and aTc were present. In the absence of one or the other, RNA Polymerase would be sterically hindered from binding to the transcription start site directly downstream of the P_{LTetO} promoter. We expected cAND to achieve signal activation only when L-ara and aTc were both present. In vivo, cAND achieved 5-fold signal activation when L-ara and aTc were present (Fig. 5C). We note there is residual activation when a single inducer is present. For cNAND, we expected loss of signal only in the presence of L-ara and aTc, and we observe a 2-fold reduction in signal only when L-ara and aTc were present (Fig. 5D). Collectively, these results demonstrate that Csr-regulated control can achieve higher order bacterial computation through two-input logic.

Employing distinct capabilities of the Csr Network to build unique genetic circuits

To further evaluate the complexity of circuitry that could be achieved using the re-purposed native Csr Network, we evaluated the ability to nest Csr-regulated two-input logic gates. To test this, we utilized the cOR Gate in tandem with a salicylic acid-inducible *eyfp* gene, to which we appended the engineered *glgC* sequence upstream of the *nahR*

https://doi.org/10.1038/s41467-024-52976-1

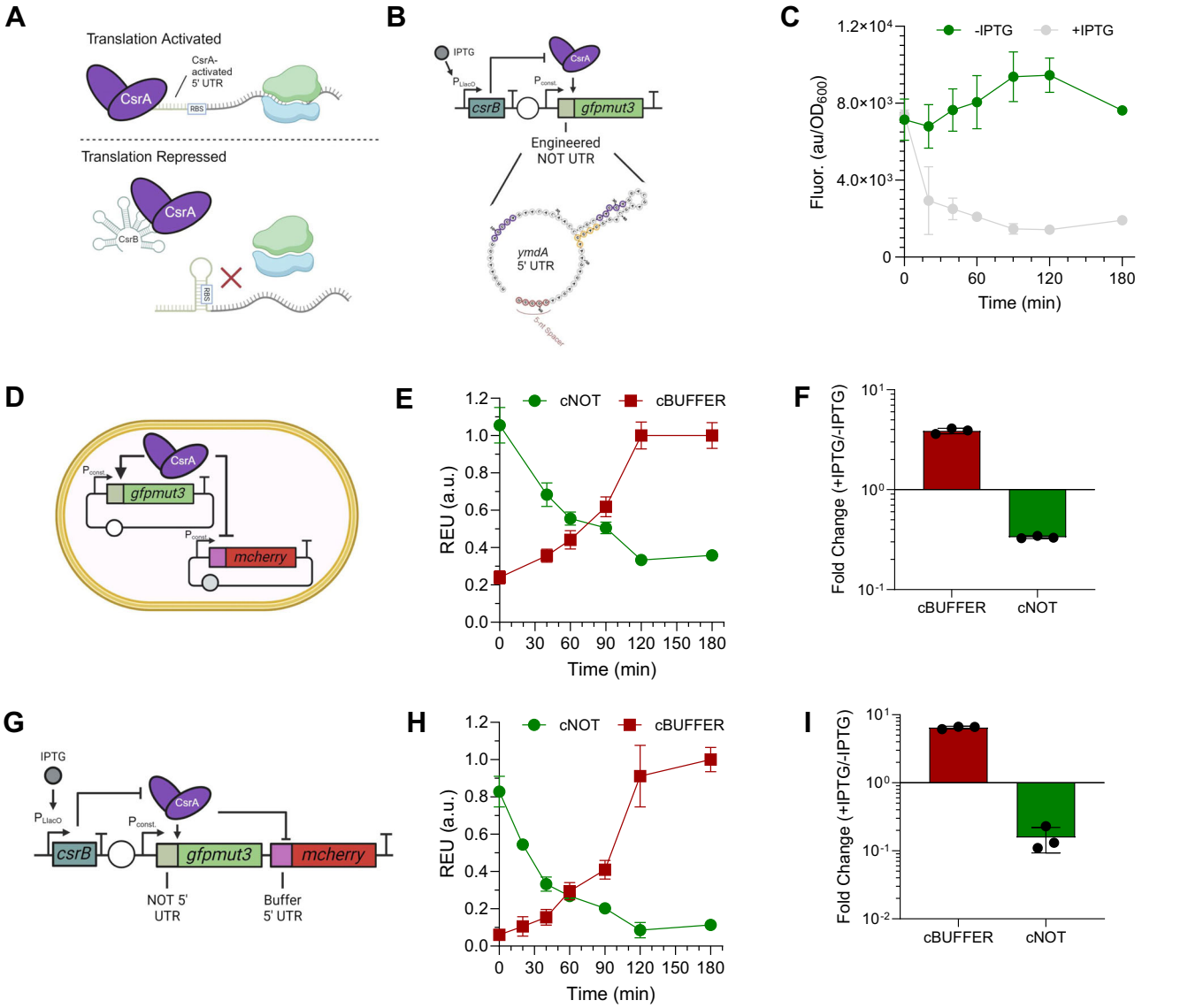

Fig. 4 | Developing a Csr-regulated NOT Gate (cNOT) and deploying in tandem with cBUFFER to engineer a bi-directional regulator. A Native regulatory interaction of the of the *ymdA* mRNA transcript with the Csr Network. In the presence of CsrA, the mRNA is bound by CsrA that activates translation. When CsrB is transcribed and sequesters CsrA, the hairpin on the CsrA, the hairpin on the *ymdA* 5′ UTR forms and prevents the ribosome from binding. **B** Genetic circuit diagram of the cNOT system - CsrA activates translation of the target gene through the engineered *ymdA* 5′ UTR. When CsrB is transcribed, it sequesters CsrA causing translation de-activation of target. **C** Time course of the cNOT fluorescence for induced and uninduced cultures. **D** Diagram of the preliminary bi-directional regulator – CsrA regulates *mcherry* via cBUFFER and *gfpmut3* via cNOT. **E** Time course of relative fluorescence for GFP and mCherry in the bi-directional using wild type CsrB. **F** Fold change of each fluorescent target two hours post-induction. **G** Genetic circuit diagram of bi-directional regulatory on a single operon. **H** Time course single operon bi-directional regulator. **I** Relative fold change of GFP and mCherry signal from the single synthetic operon bi-directional regulator two hours post-induction. Samples were grown in biological triplicate, and data presented are the mean values +/- the standard deviation, represented as the error bars.

regulator gene from the Marionette collection[31] (Fig. 5E). A CsrB and salicylic acid-dependent AND Gate was nested inside our cOR system where *eyfp* could only be induced in the presence of salicylic acid (Sal) and CsrB. Additionally, CsrB expression depended on either aTc or IPTG induction. Using this nested system, we saw a 4-fold activation in GFP signal from the cOR Gate, and 20-fold increase in EYFP signal only when CsrB and Sal were present (Fig. 5F, G), ultimately creating a three-input, two-output system capable of achieving complex bacterial computation dependent upon the rewired Csr components.

Lastly, we created a genetic pulse construct using the Csr-based regulation. To do so, we leveraged the full native Csr cascade by using the cBUFFER system in tandem with a vanillic acid-inducible[31] CsrD construct (Fig. 5H). In this circuit, CsrB sequesters CsrA away until sufficient CsrD is produced to drive degradation of the CsrB sRNA, which allows for CsrA to re-establish repression of the *gfpmut3* transcript. By inducing the CsrB sRNA and CsrD protein simultaneously, we demonstrate a Csr-regulated genetic pulse, in which GFP signal was activated then reduced by leveraging all components of the Csr Network. (Fig. 5I). Additionally, no degradation tag was required on the *gfpmut3* gene. These gates highlight the unique regulatory capabilities offered by utilizing the Csr Network as a scaffold for post-transcriptional engineering as well as highlight the complexity in bacterial computation that can be achieved through this approach.

Transporting the Csr buffer gate into bacteria containing homologous Csr network

The Csr Network is conserved across *Gammaproteobacteria* and many other classes of bacteria, particularly through the conservation of

https://doi.org/10.1038/s41467-024-52976-1

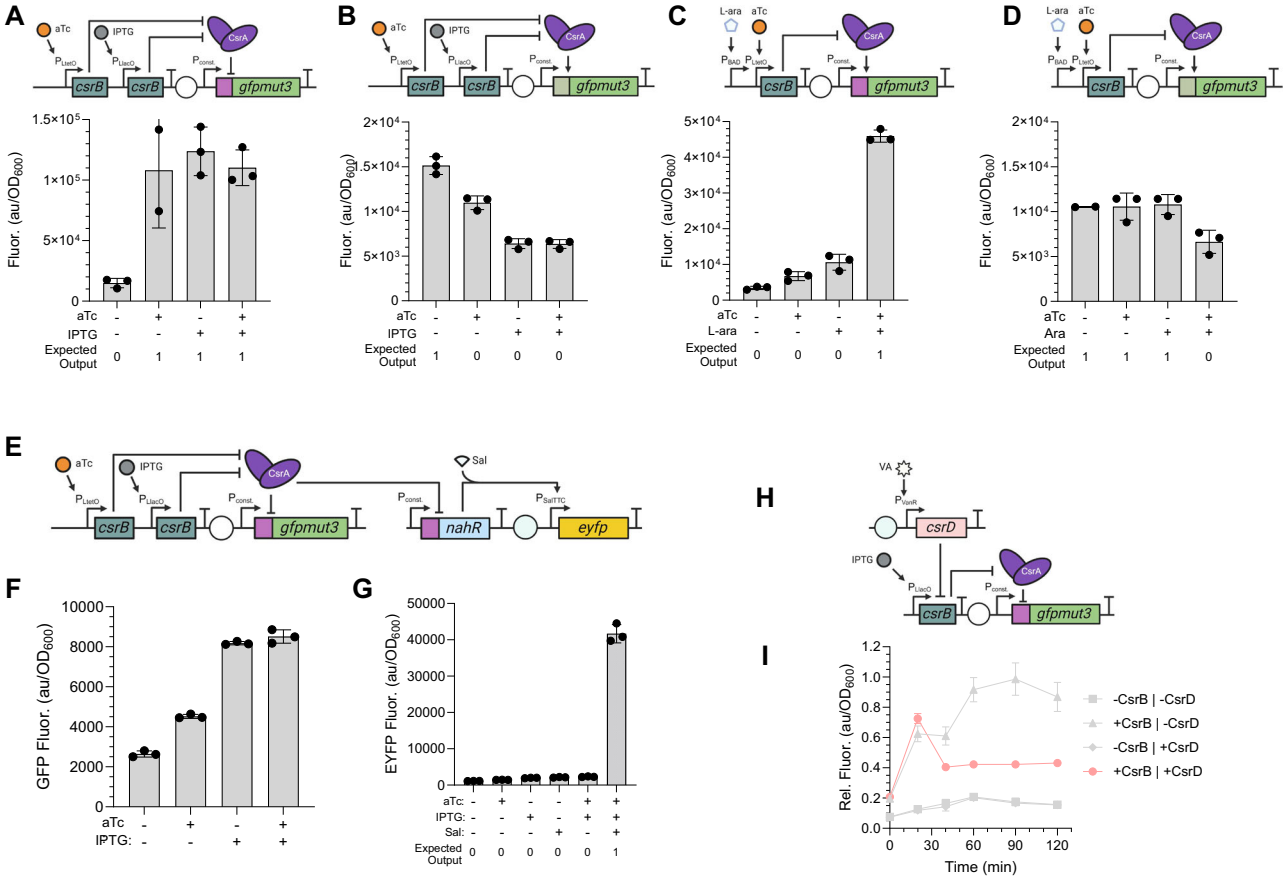

Fig. 5 | Csr-regulated Two-input and higher order logic gates. A Fluorescence of Csr-regulated OR Gate (cOR) two hours post-induction. **B** Fluorescence of Csr-regulated NOR Gate (cNOR) two hours post-induction. **C** Fluorescence of Csr-regulated AND Gate (cAND) two hours post-induction. **D** Fluorescence of Csr-regulated NANR Gate (cNAND) two hours post-induction. **E** Genetic circuit diagram of cAND inside the cOR system. The cAND system is activated when CsrB is expressed and in the presence of salicylic acid. **F** Fluorescence of cOR in nested cOR-cAND system. **G** Fluorescence of cAND in nested system. **H** Genetic circuit diagram of Csr-regulated genetic pulse. **I** Time course of genetic pulse system under different induction conditions. Samples were grown in biological triplicate, and data presented are the mean values +/- the standard deviation, represented as the error bars.

CsrA/RsmA homologous protein[12]. We therefore wanted to evaluate the modularity of the system and its transferability into organisms beyond *E. coli MG1655*. We also sought to re-establish similar regulatory capabilities by leveraging the conserved CsrA homologs. We first selected *Shewanella oneidensis MR-1* as the bacteria possess unique bioprocessing capabilities of industrial relevance[32–34] and contains a CsrA homolog. While some interactions of the homologous Csr network in *S. oneidensis* have been identified, elucidating complete biochemical mechanisms in this species is an ongoing study in the field[35]. Therefore, if we could recapitulate Csr Buffer Gate activity in *S. oneidensis* MR-1, we suspect that similar patterns would be observed in species with more well-studied Csr Networks. To ensure maximum compatibility, we replaced the original P_{Con12} constitutive promoter with ones from the Anderson Library Promoters due to their wide species versatility[36–38]. To not alter the stoichiometry between intracellular CsrA and the target mRNA transcript level, we screened several promoters and found that J23107 established the most similar response (Supplementary Figure S8). Importantly, we established that this system is tunable across multiple organisms after transforming our cBUFFER construct into MR-1 and demonstrating GFP tunability upon IPTG induction conditions in MR-1 (Fig. 6a). cBUFFER in MR-1 had a similar response function to a comparable P_{LlacO}-regulated Buffer Gate and did not exhibit any CsrB-induction dependent growth defects (Supplementary Figure S9). As a note, the LacI regulator protein derived from *E. coli* MG1655 was used as the regulator in both the cBUFFER and transcriptionally regulated gates. We then validated that cBUFFER in MR-1 was in fact CsrA-regulation dependent. To do so, we sequentially mutated the confirmed GGA motif CsrA binding sites in the engineered 5′ UTR sequence (Fig. 6b) and screened the response of each mutant. We observed a reduction in regulatory effect with each consecutive binding site mutated. When all sites were mutated, we did not observe any change in GFP fluorescence between the induced and uninduced conditions, reinforcing the homologous CsrA protein regulatory mechanisms are conserved between *E. coli* and MR-1, and the CsrA from *S. oneidensis* can recognize non-native targets in a predictable fashion (Fig. 6c).

With cBUFFER established in *S. oneidensis* MR-1, we tested the system in *Escherichia coli Nissle 1917* (EcN), and *Pseudomonas putida* KT2440 (KT2440), two gram-negative microbes that are as of industrial relevance for their therapeutic and bioprocessing applications[37,39,40]. Both species also contain CsrA homologs[41]. We also tested cBUFFER in *Bacillus subtilis* PY79 (PY79) given that it is a genetically tractable gram-positive bacterium with a CsrA homologue characterized to regulate mRNA transcripts in a similar fashion[42]. Industrial applications of *B. subtilis* focus on metabolite, and enzyme production as well as in bioremediation applications[40,43]. Of the three organisms, we observed significant cBUFFER activation upon induction in *Escherichia coli Nissle 1917*, and *Bacillus subtilis* PY79, but not in *Pseudomonas putida* KT2440 (Fig. 6e). Moreover, we observed comparable fold-changes to that of a *lacI-gfpmut3* transcriptionally regulated Buffer Gate in EcN and PY79 (Supplementary Figure S10), demonstrating that this post-transcriptional regulatory approach can

https://doi.org/10.1038/s41467-024-52976-1

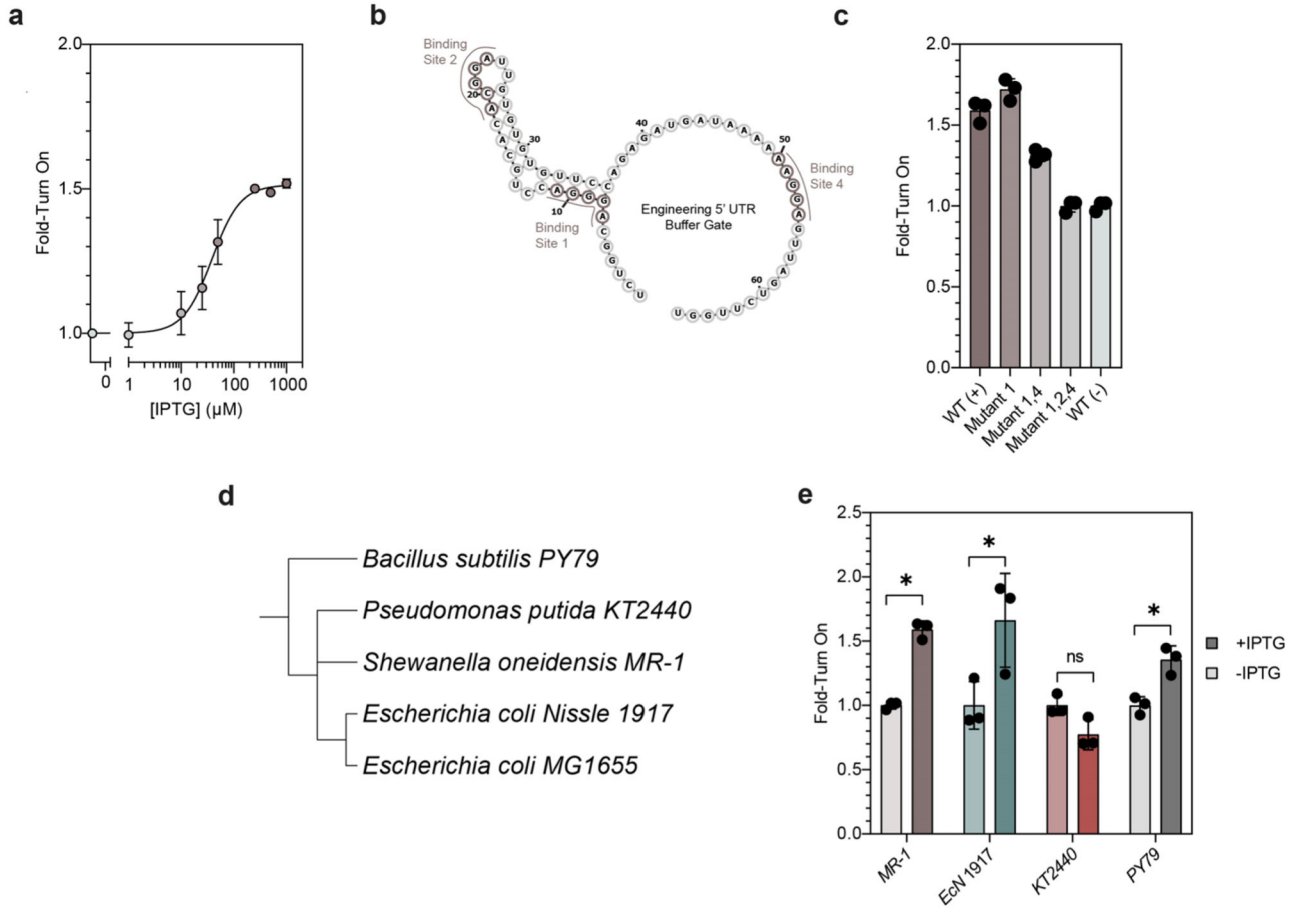

Fig. 6 | cBUFFER recapitulated in multiple industrially relevant bacteria. **a** Response function of Csr Buffer Gate in MR−1 at different IPTG induction concentrations. **b** Secondary structure of the 5′ UTR used in the Buffer Gate with each GGA binding site identified in tan. **c** Fold-Turn on of cBUFFER using the original 5′ UTR sequence, as well as 5′ UTRs with sequentially mutated CsrA binding sites. **d** Phylogenic tree of bacteria tested that contain homologous Csr/Rsm post-transcriptional networks. e Fold-turn of cBUFFER in each organism. Statistical significance was determined using two-tailed heteroscedastic t-tests between the induced and uninduced samples, in which the p-value < 0.05 (p-values for *MR-1* = 0.001, *EcN* = 0.04, *PY79* = 0.01). Samples were grown in biological triplicate, and data presented are the mean values +/- the standard deviation, represented as the error bars.

provide similar regulatory capabilities as previously established transcriptional tools[38,40]. Interestingly, we did not see activation of cBUFFER in *Pseudomonas putida* KT2440 despite its similarity to *E. coli*, while we saw activation in *Bacillus subtilis* PY79, which is more distant genetically (Fig. 6d). Importantly, the MG1655-derived LacI regulator and P_{LlacO} promoter from Lutz and colleagues[24] were used together in EcN and KT2400 for both cBUFFER and transcriptionally regulated gates. In PY79, the MG1655-derived LacI regulator was used with the P_{grac} promoter, as done in previous work[40], for both sets of BUFFER Gates.

We suspect that similar patterns will be observed in additional organisms, as the GGA binding motif has been established for other *E. coli*, *Pseudomonas*, and *Bacillus* species[43,44]. Overall, these results establish that synthetic Csr-regulated systems established in *E. coli*, with even minimal optimization, may be portable to bacteria containing homologous Csr systems and reconstituted by leveraging the conserved functions of the native CsrA proteins.

Discussion

In this work, we put forth an approach for engineered post-transcriptional genetic control by co-opting components of a global bacterial RNA regulatory network. Using the Csr Network provided the opportunity to engineer multiple regulatory handles, specifically via the CsrA and CsrD proteins and the CsrB sRNA. All components have well-defined interactions within the native Csr Network; making it a prime example to serve as a scaffold for engineered control. The components in the system inherently function together, consequently the system is natively optimized to function well in an integrated manner; this might represent an inherent advantage over de novo-designed synthetic systems. By first modulating CsrB expression, we were able to rewire CsrA to create single-input Boolean Logic Gates that utilize cognate-engineered 5′ UTRs. Then, by integrating all tunable parts of the Csr Network in concert, we demonstrate Csr-controlled higher order bacterial computation. Lastly, we port some of these interactions to other bacteria that possess a homologous network.

The Csr-regulated Buffer Gate, cBUFFER, provides tunability through three main levers: (i) inducer concentration, (ii) RBS strength, and (iii) CsrB-CsrA affinity CsrB. As CsrA natively represses and activates mRNA transcripts, we co-opted those regulatory interactions to define the identity of each logic gate based on the cognate 5′ UTR sequence (Figs. 1 and 4). To actuate the synthetic regulatory outcomes for each logic gate, we relied on the CsrB sRNA, which we showed could be precisely tuned (Fig. 2). By placing the CsrB sRNA actuator under the control of a single promoter and utilizing a combinatorial library of 5′ UTRs to control bacterial computation, we endow this system with two key advantages: access to a wider number of constitutive promoter libraries, and a reduction in required synthetic parts as circuit complexity increases. Through CsrD, we were able to add an additional layer of regulation, in which we can modulate regulator

expression, specifically by degrading the CsrB sRNA. Importantly, we were easily able to build this complex regulation without having to re-optimize each interaction between components. This feature results from co-opting a native process: the system is already optimized to work together inherently. This novelty allows for rational design of more complex regulation without requiring the optimization of multiple nested promoter and repressor pairs, which as the system complexity increases so does the risk of circuit failure[4]. It is worth noting, that other sRNAs have been characterized to co-regulate CsrA along with CsrB[16,45]; however, despite the possibility that these can add complexity to these designer circuits, this was not explored as part of this work.

Many transcriptional NOT Gates require nested repressor elements, such as those established in Wang et al.[46] in which a Lac regulatory system controls a lambda cI repressor that represses a P_R promoter regulating GFP. cNOT achieves regulation by the gene of interest being directly activated through CsrA via the engineered *ymdA* 5′ UTR and is repressed by sequestration of CsrA from the system, without additional inverter components. Only recently have transcriptional NOT Gates were developed that do not require inverters through several rounds of mutagenic screening[47]. Yet, using these native posttranscriptional regulating building blocks, we can build complex regulated logics that require less parts. First, inverting the logic within a two input Csr-regulated Gate (e.g., from OR to NOR) only requires exchanging the engineered 5′ UTR sequence. This means circuit architecture is identical between each respective gate pair (e.g., OR and NOR) and does not require additional regulatory proteins. The identical circuit architecture is achieved by eliminating the need for additional nested repressors, and results in overall circuit compression. Beyond two-input gates, there are several instances, in which repurposing native Csr regulation creates efficient and complex genetic circuits. Since regulation in the Csr Network has multiple well-defined protein-RNA interactions, there are multiple instances to design circuits with increased complexity without having to completely re-engineer the system or combine multiple independent components. As a key example, our scheme allows for diverging regulatory outcomes within a single operon (Fig. 4G–I) by changing only the engineered UTR upstream of each target gene. This design provides unique opportunities to regulate pathways in a single synthetic operon, whereby individual logic can be controlled individually via UTR engineering. A potential application of these types of design is two-stage fermentation for value-added chemical production. In the first stage, pathways that drive biomass accumulation are upregulated. Once the culture receives a specific environmental signal, the second stage begins, shutting off all biomass and upregulating the specific metabolic pathway for the desired molecule[48]. The bi-directional regulator in this work would allow for consolidation of both pathways to be regulated by native levels of CsrA and activated through a single synthetic actuator in CsrB. This highlights the benefits of native and synthetic components working synergistically with each other.

Building on our logical complexity, we were able to nest an AND Gate inside of a cOR system by fusing the engineered *glgC* 5′ UTR directly upstream of a salicylic acid-inducible regulator *nahR*, such that that activation required both CsrB expression and salicylic acid induction (Fig. 5E–G). This created a Csr-derived construct to recognize three input signals and process two separate outputs, in our case GFPmut3 and EYFP. Moreover, the Sal-based AND Gate achieved circuit compression by only requiring four synthetic parts, while a traditional Cello-based AND Gate still requires 6 parts, and a nested OR-AND system would require an even larger number of proteins. Additionally, the Csr-regulated circuits reduces total nucleotides required to achieve the same function as other similar genetic circuits. Using less nucleotides overall can facilitate the need for less cellular burden and for less resources required, such as free nucleotides.

Demonstrating that Csr-regulated genetic circuits can be integrated with established transcriptionally regulated systems is a promising foundation for developing complex genetic circuits (Fig. 5E–G). In future versions of Csr-regulated system, developing orthogonal CsrA-RNA binding motifs would be valuable for increasing circuit complexity. In the current version of Csr-regulated genetic circuits, once CsrB expression is induced, the downstream regulatory functions are executed. Using multiple orthogonal systems would avoid that limitation and allow for more complex layering of genetic circuits so that users could precisely control both expression and regulatory outcome for each gene independently. This technology could be useful in metabolic engineering applications. Lastly, implementing degradation of the CsrB RNA by the CsrD protein provides the ability to return the system to its original state by controlling the reduction of cellular concentrations of CsrB, providing access to high-order bacterial computation. Integrating CsrD provides the ability to "undo" the regulatory effect of CsrB and adds another tunable element to the system. This sets the stage for even more complex bacterial computation such as IMPLY, NIMPLY, XOR, or XNOR functions. By co-opting the process of CsrD-driven degradation of CsrB, we can create a Csr-based pulse-generating circuit (Fig. 5H, I). The native interactions between CsrD and CsrB allow for both activation, and subsequent deactivation, with a fold-activation response similar to previously established transcriptionally regulated pulse-generating circuits[6,49]. Moving forward, it may be useful to further explore the tunability between CsrD and CsrB interactions to see how modulating those interacts affects the response of the pulse-generating circuit. Additionally, our current system utilizes two inputs, while previous works have leveraged one-input incoherent feedforward loops[6,49]. In future versions of the Csr-regulated pulse-generating circuit, it may be beneficial to develop a system that relies on a single input to reduce the number of synthetic components required, as well as ensure simultaneous induction of CsrB and CsrD. These results support the notion that an engineered Csr system is capable of high-level bacterial computation with streamlined circuit design and more modular engineering handles.

As the Csr Network is conserved across most *Gammaproteobacteria* as well as other classes of bacteria, there are many potential organisms of industrial relevance that could utilize this regulatory scheme[50]. In our work, we demonstrated the Csr-regulated Buffer Gate can be recapitulated in *S. oneidensis* MR-1, *E. coli Nissle 1917* (EcN), and *B. subtilis* (Fig. 6e) and achieve similar levels of fold-regulation to their transcriptional Buffer Gate counterparts (Supplementary Figure S10). Importantly, we utilized the engineered 5′ UTR sequence as well as the CsrB sRNA sequenced from *E. coli* and still were able to establish regulation, which alludes to the fact that the natively expressed CsrA homolog in each organism can interact with the non-native transcripts. This is particularly interesting for *B. subtilis*, as no CsrB sRNA homolog has been experimentally validated. Additionally, through our mutational analysis (Fig. 6c) we demonstrated that the CsrA homolog in *S. oneidensis* appears to follow the same regulatory mechanism of the engineered 5′ UTR to that of the CsrA native to *E.* coli. This highlights that this scheme opens a much larger design space throughout and across bacterial species. This may become relevant when moving into organisms where few promoters are characterized as few inducible promoters are required to actuate complex logic. Additionally, as these systems rely on native components from a well-conserved network, they may be less likely to fail when ported to another organism, a major concern in de novo engineered bacterial circuits[51,52]. As such, this work effectively recapitulates adaptation of post-transcriptional Buffer Gates on heterologous targets across multiple industrially relevant species.

Methods

Bacterial strains and growth conditions

All strains of *E. coli* used in the single- and multi-input gate are derived from K-12 MG1655. The DH5α strain was used for all plasmid cloning.

S. oneidensis MR-1, *P. putida* KT2440, *E. coli Nissle* 1917, and *B. subtilis* PY79 were used for the experiments that ported the Csr-regulated Buffer Gate into other bacterial species. The full genotype of each strain used in this work can be found in the Supplementary Materials and Methods. *E. coli* strains used in the single- and multi-input gate were cultured in LB Medium (Miller) (BD Biosciences) supplemented with 100 µg/mL Carbenicillin, and/or 50 µg/mL Kanamycin, and or/ 34 µg/mL Chloramphenicol, as necessary. Seed cultures were grown overnight at 37 °C in an orbital shaking incubator (New Brunswick Scientific *I26*). Cultures were prepared by inoculating 5 mL samples of LB plus the appropriate antibiotics with a single colony of the respective *E. coli* strain grown on LB Agar (Fisher Bioreagents) + appropriate antibiotics. Single- and multi-input gate experiments, overnight cultures were diluted 1:100 into 30 mL LB + antibiotics and grown in the 37 °C shaking incubator. Samples were also grown in the 37 °C shaking incubator. All samples were induced with variable concentrations of isopropyl β-D-1-thiogalactopyranoside (IPTG), anhydrotetracycline (aTc), or L-arabinose (L-ara). Stocks of IPTG and were prepared in UltraPure™ Distilled Water (invitrogen), and stocks of aTc were prepared in a 1:1 mixture of UltraPure™ Distilled Water and OmniPur 200 Proof Ethyl Alcohol (Calbiochem, Sigma-Aldrich). Information growth conditions for *S. oneidensis* MR-1, *P. putida* KT2440, *E. coli Nissle* 1917, and *B. subtilis* PY79 can be found in the supplemental materials and methods.

Plasmid construction

All plasmids used in this study are provided in Supplementary Table S1. All plasmids were constructed using Gibson Assembly. Oligonucleotide primers and gBlocks were purchased from Integrated DNA Technologies (IDT) and are provided in Supplementary Table S2. Gibson assembly primers were designed as follows: annealing region was designed to include 15–25 nucleotides (nt) of homology to the parent plasmid. The Gibson overhang region was at least 16 nucleotides in length. Primers were designed to minimize GC content, and the homodimer ΔG energy was greater than -18 kcal/mol, as estimated by the IDT OligoAnalyzer (https://www.idtdna.com/calc/analyzer). Plasmids were verified for sequencing by Sanger Sequencing (University of Texas GSAF core) and Plasmidsaurus (https://www.plasmidsaurus.com/). Plasmids derived from previous work was sequence confirmed and analyzed by both Plasmidsaurus and Plannotate (McGuffie,M.J. and Barrick,J.E. 2021 *NAR* http://plannotate.barricklab.org/)[53]. It is important to note that the pMP11 plasmid was a generous gift from the lab of Professor Brian Pfleger at the University of Wisconsin-Madison and was used for CRISPR-Cas9-based genome editing of *E. coli* following previously established protocols[54,55]. Additionally, the pCG004 plasmid was a generous gift from Professor Aditya Kunjapur from the University of Delaware and was a parent plasmid for cloning the Csr-regulated Buffer Gate into a *B. subtilis*-compatible vector.

Strain construction

The MG1655 *ΔcsrBΔcsrCΔcsrD E. coli* strain was constructed following the CRISPR-Cas9 protocol previously developed[54,55]. To summarize, the method uses a 2-plasmid system; the first plasmid (sgRNA-*csrD*) contains a constitutively expressed sgRNA that targets the genomic region of *csrD*, the second (pMP11) contains a constitutively expressed *S. pyogenes* Cas9 protein, an L-arabinose-inducible lambda-red recombinase system, an aTc-inducible sgRNA that targets the first plasmid, and a temperature sensitive origin of replication. The csrD gRNA sequence was selected using the CRISPR gRNA Design webtool from Atum (atum.bio). The knockout was made as follows: pMP11 was electroporated (Supplemental Materials and Methods) into an MG1655 *ΔcsrBΔcsrC* strain of *E. coli* from Sowa et al. 2017 and electrocompetent cells were prepared as follows: an overnight starter culture was diluted 1:100 into 50 mL of LB + carbenicillin and grown at 30 °C in the shaking incubator. After 1 hour, 2.5 mL of 20% L-arabinose was added to the culture, for a final concentration of 1% L-arabinose, to induce the lambda-red genes. Once the cells reached an OD_{600} of 0.5, they were put on ice, and spun down at ~2000xg for 10 minutes at 4 °C and the supernatant was discarded. The cells were washed with 45 mL of 10% glycerol solution and spun down again at the same conditions. The wash steps were repeated with 25 mL and 10 mL of the 10% glycerol solution. The final pellet was resuspended in 500 µL of 10% glycerol and aliquoted into 50 µL samples. An aliquot of competent cells was mixed with 100 ng of purified pgRNA plasmid and 1 µL of a 60 nt oligo that contains 30 nt upstream of the *csrD* gene and 30 nt downstream of *csrD*. Plasmid and oligo were electroporated and cells were recovered in 900 µL of SOB (Supplemental Materials and Methods) for 3 hours at 30 °C and plated on LB Agar plates with appropriate antibiotics. Single colonies were selected the next day and analyzed via cPCR for successful gene knockout. Successful knockouts were grown in an overnight starter culture at 30 °C with aTc to cure the pgRNA-*csrD* plasmid. The following day, the cells were grown on LB Agar + antibiotics plate and screened for successful pgRNA curing. Once the pgRNA was cured, single colonies were struck on LB Agar plates and grown overnight at 42 °C to cure out pMP11. Individual colonies were screened for curing of pMP11 by streaking colonies on LB Agar and LB Agar + Carbenicillin plates and grown at 30 °C overnight.

Single- and Multi-Input Gate Fluorescence Assays

The response of the Csr-regulated single- and multi-input gates was tested in biological triplicate, and each gate was analyzed using cultures grown in 250 mL flasks. To prepare samples, overnight cultures single colonies of the *E. coli* strain containing the Csr-regulated Logic Gate plasmid were inoculated into a 5 mL of LB plus the appropriate antibiotic and grown overnight at 37 °C in a shaking incubator. The next day, the overnight culture was diluted 1:100 in 30 mL of LB plus the respective antibiotic. Samples were grown in a shaking incubator at 37 °C. After two hours of growth, which corresponded to an OD_{600} between 0.18–0.35, samples were induced with IPTG, aTc, or L-arabinose. For the single-input logic gate experiments, samples were induced with 30 µL of 500 mM IPTG for a final concentration of 500 µM IPTG. For multi-input gate experiments, samples were induced with 30 µL of 500 mM IPTG and 30 µL of 100 µg/mL aTc or 30 µL of 100 µg/mL aTc and 30 µL of 20% L-arabinose. After induction fluorescence and OD_{600} were tracked over time using a BioTek Cytation3 plate reader. At each timepoint, 50 µL of cell culture was diluted into 150 µL of 1x PBS, then fluorescence and OD_{600} were measured. 50 µL of LB was used as a blank. To measure *gfpmut3* fluorescence, excitation and emission wavelengths of 488 nm and 515 nm with a gain of 80. *Mcherry* fluorescence was measured using excitation and emission wavelengths of 585 nm and 613 nm with a gain of 85. *eypf* fluorescence was measured using an excitation and emission wavelengths of 500 nm and 530 nm with a gain of 70. OD_{600} was measuring absorbance using a wavelength of 600 nm.

Calculating fluorescence expression (Fl/OD_{600})

Fluorescence was calculated by dividing the normalized sample fluorescence, calculated by subtracting the fluorescence of cultures containing an empty plasmid from the raw fluorescence of the sample cultures, by the normalized OD_{600} (Fl/OD) of each sample The full equation to calculate Fl/OD_{600} is as follows:

$$Fl/OD = \frac{Raw\ Sample\ Fluorescence\,(au.u) - Control\ Sample\,(a.u.)}{Abs.\,(600nm) of\ Sample - Abs.\,(600nm) of\ media}$$

Calculating relative expression units (REU)

Relative Expression Units (REU) was implemented primarily when comparing system activation between two different regulatory constructs, such as in Supplementary Figure S2 or when comparing relative expression for multiple proteins. REU is calculated by dividing the Fluorescence normalized by OD_{600} (Fl/OD) measured from the samples grown in the testing strain (either MG1655 or MG1655 *ΔcsrBΔcsrCΔcsrD*) by that of the Fl/OD of the samples grown in a *csrA* knockdown strain (*csrA::kan)*. As a note, *csrA* cannot be fully knocked out from the genome, but inserting the *kan* cassette reduced CsrA activity by 87%. The full Eq. (1) to calculate REU is as follows:

$$REU = \frac{\frac{Fluorescence\,(a.u.)}{OD_{600}\,(Abs\ at\ 600\ nm)}\ of\ sample\ in\ testing\ strain}{\frac{Fluorescence\,(a.u.)}{OD_{600}\,(Abs\ at\ 600\ nm)}\ of\ sample\ in\ csrA::kan\ strain} \quad (1)$$

Reporting summary

Further information on research design is available in the Nature Portfolio Reporting Summary linked to this article.

Data availability

Sequences for plasmids used in this study are provided in the Supplementary Information. Materials generated in this study are available upon request. Source data are provided with this paper.

References

1. Engineering Biology Research Consortium (2023). An Assessment of Short-Term Milestones in EBRC's 2019 Roadmap, Engineering Biology. https://doi.org/10.25498/E4NP46.
2. Glick, B. R. Metabolic load and heterologous gene expression. *Biotechnol. Adv.* **13**, 247–261 (1995).
3. Kurland, C. G. & Dong, H. Bacterial growth inhibition by overproduction of protein. *Mol. Microbiol.* **21**, 1–4 (1996).
4. Brophy, J. A. N. & Voigt, C. A. Principles of genetic circuit design. *Nat. Methods* **11**, 508–520 (2014).
5. Frumkin, I. et al. Gene Architectures that Minimize Cost of Gene Expression. *Mol. Cell* **65**, 142–153 (2017).
6. Westbrook, A. et al. Distinct timescales of RNA regulators enable the construction of a genetic pulse generator. *Biotechnol. Bioeng.* **116**, 1139–1151 (2019).
7. Takahashi, M. K. et al. Rapidly Characterizing the Fast Dynamics of RNA Genetic Circuitry with Cell-Free Transcription–Translation (TX-TL) Systems. *ACS Synth. Biol.* **4**, 503–515 (2015).
8. Ceroni, F. et al. Burden-driven feedback control of gene expression. *Nat. Methods* **15**, 387–393 (2018).
9. Pfleger, B. F., Pitera, D. J., Smolke, C. D. & Keasling, J. D. Combinatorial engineering of intergenic regions in operons tunes expression of multiple genes. *Nat. Biotechnol.* **24**, 1027–1032 (2006).
10. Na, D. et al. Metabolic engineering of Escherichia coli using synthetic small regulatory RNAs. *Nat. Biotechnol.* **31**, 170–174 (2013).
11. Cho, J. S. et al. Targeted and high-throughput gene knockdown in diverse bacteria using synthetic sRNAs. *Nat. Commun.* **14**, 2359 (2023).
12. Vakulskas, ChristopherA., Potts, AnastasiaH., Babitzke, Paul, Ahmer, BrianM. M. & Romeo Tony. Regulation of Bacterial Virulence by Csr (Rsm) Systems. *Microbiol. Mol. Biol. Rev.* **79**, 193–224 (2015).
13. Sowa, S. W. et al. Integrative FourD omics approach profiles the target network of the carbon storage regulatory system. *Nucleic Acids Res.* **45**, 1673–1686 (2017).
14. Leistra, A. N. et al. A Canonical Biophysical Model of the CsrA Global Regulator Suggests Flexible Regulator-Target Interactions. *Sci. Rep.* **8**, 9892 (2018).
15. Potts, A. H. et al. Global role of the bacterial post-transcriptional regulator CsrA revealed by integrated transcriptomics. *Nat. Commun.* **8**, 1596 (2017).
16. Rojano-Nisimura, A. M. et al. CsrA selectively modulates sRNA-mRNA regulator outcomes. *Front. Mol. Biosci.* **10**, (2023).
17. Dubey, A. K., Baker, C. S., Romeo, T. & Babitzke, P. RNA sequence and secondary structure participate in high-affinity CsrA–RNA interaction. *RNA* **11**, 1579–1587 (2005).
18. Baker, C. S., Morozov, I., Suzuki, K., Romeo, T. & Babitzke, P. CsrA regulates glycogen biosynthesis by preventing translation of glgC in Escherichia coli. *Mol. Microbiol.* **44**, 1599–1610 (2002).
19. Weilbacher, T. et al. A novel sRNA component of the carbon storage regulatory system of Escherichia coli. *Mol. Microbiol.* **48**, 657–670 (2003).
20. Leng, Y. et al. Regulation of CsrB/C sRNA decay by EIIAGlc of the phosphoenolpyruvate: carbohydrate phosphotransferase system. *Mol. Microbiol.* **99**, 627–639 (2016).
21. Zere, T. R. et al. Genomic Targets and Features of BarA-UvrY (-SirA) Signal Transduction Systems. *PLOS ONE* **10**, e0145035 (2015).
22. Liu, M. Y., Yang, H. & Romeo, T. The product of the pleiotropic Escherichia coli gene csrA modulates glycogen biosynthesis via effects on mRNA stability. *J. Bacteriol.* **177**, 2663–2672 (1995).
23. Adamson, D. N. & Lim, H. N. Rapid and robust signaling in the CsrA cascade via RNA–protein interactions and feedback regulation. *Proc. Natl. Acad. Sci.* **110**, 13120–13125 (2013).
24. Lutz, R. & Bujard, H. Independent and Tight Regulation of Transcriptional Units in Escherichia Coli Via the LacR/O, the TetR/O and AraC/I1-I2 Regulatory Elements. *Nucleic Acids Res* **25**, 1203–1210 (1997).
25. Vakulskas, C. A. et al. Antagonistic control of the turnover pathway for the global regulatory sRNA CsrB by the CsrA and CsrD proteins. *Nucleic Acids Res.* **44**, 7896–7910 (2016).
26. Leistra, A. N., Amador, P., Buvanendiran, A., Moon-Walker, A. & Contreras, L. M. Rational Modular RNA Engineering Based on In Vivo Profiling of Structural Accessibility. *ACS Synth. Biol.* **6**, 2228–2240 (2017).
27. Salis, H. M. Chapter two - The Ribosome Binding Site Calculator. in *Methods in Enzymology* (ed. Voigt, C.) vol. 498 19–42 (Academic Press, 2011).
28. Renda, A. et al. CsrA-Mediated Translational Activation of ymdA Expression in Escherichia coli. *mBio* **11**, https://doi.org/10.1128/mbio.00849-20 (2020).
29. Beck, C. F., Mutzel, R., Barbé, J. & Müller, W. A multifunctional gene (tetR) controls Tn10-encoded tetracycline resistance. *J. Bacteriol.* **150**, 633–642 (1982).
30. Johnson, C. M. & Schleif, R. F. In vivo induction kinetics of the arabinose promoters in Escherichia coli. *J. Bacteriol.* **177**, 3438–3442 (1995).
31. Meyer, A. J., Segall-Shapiro, T. H., Glassey, E., Zhang, J. & Voigt, C. A. Escherichia coli "Marionette" strains with 12 highly optimized small-molecule sensors. *Nat. Chem. Biol.* **15**, 196–204 (2019).
32. Partipilo, G., Graham, A. J., Belardi, B. & Keitz, B. K. Extracellular Electron Transfer Enables Cellular Control of Cu(I)-Catalyzed Alkyne–Azide Cycloaddition. *ACS Cent. Sci.* **8**, 246–257 (2022).
33. Gao, Y. et al. A hybrid transistor with transcriptionally controlled computation and plasticity. *Nat. Commun.* **15**, 1598 (2024).
34. Wang, T. et al. Developing a PAM-Flexible CRISPR-Mediated Dual-Deaminase Base Editor to Regulate Extracellular Electron Transport in Shewanella oneidensis. *ACS Synth. Biol.* **12**, 1727–1738 (2023).
35. Binnenkade, L., Lassak, J. & Thormann, K. M. Analysis of the BarA/UvrY Two-Component System in Shewanella oneidensis MR-1. *PLOS ONE* **6**, e23440 (2011).
36. Anderson, J. C. et al. BglBricks: A flexible standard for biological part assembly. *J. Biol. Eng.* **4**, 1 (2010).

37. Rottinghaus, A. G., Ferreiro, A., Fishbein, S. R. S., Dantas, G. & Moon, T. S. Genetically stable CRISPR-based kill switches for engineered microbes. *Nat. Commun.* **13**, 672 (2022).
38. Cook, T. B. et al. Genetic tools for reliable gene expression and recombineering in Pseudomonas putida. *J. Ind. Microbiol. Biotechnol.* **45**, 517–527 (2018).
39. Praveschotinunt, P. et al. Engineered E. coli Nissle 1917 for the delivery of matrix-tethered therapeutic domains to the gut. *Nat. Commun.* **10**, 5580 (2019).
40. Stork, D. A. et al. Designing efficient genetic code expansion in Bacillus subtilis to gain biological insights. *Nat. Commun.* **12**, 5429 (2021).
41. Altegoer, F., Rensing, S. A. & Bange, G. Structural basis for the CsrA-dependent modulation of translation initiation by an ancient regulatory protein. *Proc. Natl. Acad. Sci.* **113**, 10168–10173 (2016).
42. Mukherjee, S. et al. CsrA–FliW interaction governs flagellin homeostasis and a checkpoint on flagellar morphogenesis in Bacillus subtilis. *Mol. Microbiol.* **82**, 447–461 (2011).
43. Sun, Z., Zhou, N., Zhang, W., Xu, Y. & Yao, Y.-F. Dual role of CsrA in regulating the hemolytic activity of Escherichia coli O157:H7. *Virulence* **13**, 859–874 (2022).
44. Pourciau, C., Lai, Y.-J., Gorelik, M., Babitzke, P. & Romeo, T. Diverse Mechanisms and Circuitry for Global Regulation by the RNA-Binding Protein CsrA. *Front. Microbiol.* **11**, (2020).
45. Jørgensen, M. G., Thomason, M. K., Havelund, J., Valentin-Hansen, P. & Storz, G. Dual function of the McaS small RNA in controlling biofilm formation. *Genes Dev* **27**, 1132–1145 (2013).
46. Wang, B., Kitney, R. I., Joly, N. & Buck, M. Engineering modular and orthogonal genetic logic gates for robust digital-like synthetic biology. *Nat. Commun.* **2**, 508 (2011).
47. Groseclose, T. M., Rondon, R. E., Herde, Z. D., Aldrete, C. A. & Wilson, C. J. Engineered systems of inducible anti-repressors for the next generation of biological programming. *Nat. Commun.* **11**, 4440 (2020).
48. Burg, J. M. et al. Large-scale bioprocess competitiveness: the potential of dynamic metabolic control in two-stage fermentations. *Curr. Opin. Chem. Eng.* **14**, 121–136 (2016).
49. Tickman, B. I. et al. Multi-layer CRISPRa/i circuits for dynamic genetic programs in cell-free and bacterial systems. *Cell Syst.* **13**, 215–229.e8 (2022).
50. Romeo, T. & Babitzke, P. Global Regulation by CsrA and Its RNA Antagonists. *Microbiol. Spectr.* **6**, 10.1128/microbiolspec.rwr-0009–2017 (2018).
51. Cardinale, S. & Arkin, A. P. Contextualizing context for synthetic biology – identifying causes of failure of synthetic biological systems. *Biotechnol. J.* **7**, 856–866 (2012).
52. Kittleson, J. T., Wu, G. C. & Anderson, J. C. Successes and failures in modular genetic engineering. *Curr. Opin. Chem. Biol.* **16**, 329–336 (2012).
53. McGuffie, M. J. & Barrick, J. E. pLannotate: engineered plasmid annotation. *Nucleic Acids Res.* **49**, W516–W522 (2021).
54. Hernández Lozada, N. J. et al. Highly Active C8-Acyl-ACP Thioesterase Variant Isolated by a Synthetic Selection Strategy. *ACS Synth. Biol.* **7**, 2205–2215 (2018).
55. Mehrer, C. R., Incha, M. R., Politz, M. C. & Pfleger, B. F. Anaerobic production of medium-chain fatty alcohols via a β-reduction pathway. *Metab. Eng.* **48**, 63–71 (2018).

Acknowledgements

This work was financially supported by the National Science Foundation [grant numbers MCB-1932780 to L.M.C., A.S., and R.B.] the National Institutes of Health [grant number R35GM133640 to B.K.K. and D.C.], the Welch Foundation [grant number F-1929 to B.K.K, and D.C.], and an NSF CAREER Award [1944334 to B.K.K.]. T.R.S. and G.P. were supported through National Science foundation Graduate Research Fellowships [program award number DGE-1610403]. A.S. was also financially supported through an Undergraduate Research Fellowship from the Office of Undergraduate Research at the University of Texas at Austin. We would like to thank Michaela A. Jones and Dr. Aditya M. Kunjapur from the University of Delaware for generously providing the pCG004 construct and valuable insight on methods to optimize transformation efficiency in *B. subtilis*. We would also like to thank the lab of Dr. Brian Pfleger from the University of Wisconsin-Madison for providing the pMP11 and pgRNA constructs and helpful protocols on CRISPR-Cas9-based recombineering in *E. coli*. We would also like to thank the members of the Contreras Lab for their helpful discussions during the development of this work. Some images were made using BioRender and can be accessed at the following links: Fig. 1 (BioRender.com/z27r836), Fig. 2 (BioRender.com/x78f681), Fig. 3 (BioRender.com/v46c495), Fig. 4 (BioRender.com/q60b129), Fig. 5 (BioRender.com/f68j100). Data were visualized using GraphPad Prism.

Author contributions

T.R.S., G.P., R.B., A.C.S, B.K.K., and L.M.C. designed the experimental research. T.R.S., G.P., A.C.S., R.S., and D.C. performed the experiments, T.R.S., G.P., and A.C.S., analyzed the data and prepared the corresponding figures. T.R.S., G.P., A.C.S., and L.M.C. wrote the manuscript. T.R.S., G.P., R.B., A.C.S., B.K.K., and L.M.C. edited and reviewed the manuscript. All authors have given approval to the final version of this manuscript.

Competing interests

The authors declare no competing interests

Additional information

Supplementary information The online version contains supplementary material available at https://doi.org/10.1038/s41467-024-52976-1.

Correspondence and requests for materials should be addressed to Lydia M. Contreras.

Peer review information *Nature Communications* thanks the anonymous reviewers for their contribution to the peer review of this work. A peer review file is available.